An Experimentally Verified Methodology for Calculating Coaxial Cable Loss Effects on CDM Waveforms

Peyman Ensaf (1), Timothy J. Maloney (2)

(1) Intel Corp., 2501 NE Century Blvd, Hillsboro, OR 97124 USA
tel.: 503-754-8981, e-mail: peyman.ensaf@intel.com

(2) Center for Analytic Insights, Palo Alto, CA USA

e-mail: tjmaloney@sbcglobal.net

Abstract - Experimental verification of a turnkey methodology for assessing the precise impact of cable loss on specified CDM pulses in the time domain is presented. Experiments verify the impact of cable losses, mainly skin depth, by convolving CDM waveforms with impulse responses for cables of various lengths.

I. Introduction

The CDM (Charged Device Model) tester measurement channel is described in the test standard [1] and has three main elements for capturing a voltage waveform approximating the device current: Fast oscilloscope, high-speed cables, and a test head with a current-sensing 1-ohm resistor. Performance expectations for these three sections, and other hardware, are described in the standard. The effect of oscilloscopes on CDM waveforms was treated at this conference in 2011 [2]. Fortunately, scopes have improved so that 6 GHz bandwidth is now common and are preferred in [1] for system verification. Major corrections to verification waveforms are known and would not be substantial but corrections could be made if needed.

This paper will focus on the second measurement element, the coaxial cables (about 2 meters) that transport the test head signal to the scope. In the 2018 version [1], this cable assembly is required to have less than 2 dB loss at 5 GHz. The earlier 2014 version specified the same loss at 9 GHz, but after some informal studies of cables actually used [3,4], the spec was adjusted in order to be achievable with fast cables in common use, cables that still had acceptably small losses. This paper develops a method to find the exact transformation of the test head signal by the cables, a filter function that can correct the entire measured waveform for cable losses and, if desired, be combined with the scope filter function. Comments on the test head corrections, the third measurement element, appear near the end of this paper.

This paper's objective is to confirm, through experiments, that the formation of cable filter functions and waveform correction as in [4] is correct and workable. This study used time domain filter functions for an Excel worksheet using numerical convolution. References [3,4] used datasheet values of cable loss for the analysis, but here we augment that with our own network analyzer loss measurements. These allow comparison with datasheet values and give parameters for use in formulating a final filter function for the cable assembly. Before we look at high-speed cables actually used on CDM testers, where losses are mild and only weakly affect the waveform, as hoped, we will confirm the analytic methods with lengths of lossier cable that provide more loss signal and more accurate comparison of theory to experiment in pulse measurements. Then, after our analysis of typical high-speed cables used in CDM testers, we will present a simple chart for everyday use, one that estimates the peak current correction well for a pulse of a given width. The goal of this paper is that a user can largely benefit from this study without having to adopt all its analysis and waveform correction methods.

Dielectric [5] and skin depth losses [6] have long been studied in transmission lines. Skin depth losses far exceed the dielectric losses at RF frequencies up to 5 GHz and were the sole focus of the oldest study [6]. Skin depth and dielectric losses are described by the impulse responses $h_1(t)$ and $h_2(t)$ respectively shown in equations 1 and 2, from [4] and earlier references [5,6]. Both $h_1(t)$ and $h_2(t)$ integrate over time to unity, as dc losses are negligible.

$$h_1(t) = \frac{\sqrt{\tau_1}}{2t\sqrt{\pi t}} e^{\frac{-\tau_1}{4t}} \quad Skin\ effect \qquad (1)$$

$$h_2(t) = \frac{2\tau_2}{\pi(\tau_2^2 + t^2)} \quad Dielectric\ loss \quad (2)$$

Where t is time and τ_1 and τ_2 (seconds) [3,4] are functions of quantities a and b from a second order fit, dB=a$\sqrt{f}$+bf, f=frequency in MHz, as shown in Equations 3 and 4. Curve fits come from Figures 3 & 4, later.

$$\tau_1 = \frac{\ln^2 10}{400\pi}\, a^2 * 10^{-6} \quad (sec) (3)$$

$$\tau_2 = \frac{\ln 10}{20\pi}\, b * 10^{-6} \quad (sec) \quad (4)$$

The coefficient a has units of 1/square root (frequency) and b is just a number in micro-seconds. τ_1 and τ_2 are in pico-seconds for the purposes of numerical calculations. It is comforting that the curve-fit quantities a and b are occasionally listed in a cable manufacturer's datasheet of dB/m losses over frequency. Equations 3 and 4 are usually calculated for a 1-meter long length of coaxial cable, however coefficients a and b can simply be scaled up for longer cables. Furthermore, note that skin depth loss goes as square root of frequency while dielectric loss goes with frequency. Convolving equations 1 and 2 [4,5] will result in a third impulse response $h_3(t)$ which has the contribution of both skin and dielectric losses shown in Equation 5.

$$h_3(t) = \int_0^t h_2(t-\tau) h_1(\tau) d\tau \quad (5)$$

$$or\ h_3(t) = h_1(t) \otimes h_2(t)\ Convolution \quad (6)$$

Equations 5 and 6 are identical, only the symbol $\otimes$ in Equation 6 is a shorthand representation of the convolution integral, and in this case of the two impulse responses corresponding to skin and dielectric losses. The commonly used symbol $\otimes$ will be used henceforth. Impulse response $h_3(t)$ in Equation 6 is then convolved with a CDM reference waveform. Since $h_3(t)$ from Equation 5 incorporates both skin and dielectric losses, once convolved with the input (or CDM reference waveform), the resulting waveform will be the attenuated version of the pulse at the scope (after passing through a length of cable).

II. Measurement Techniques

This technique relies on being able to measure two channels of the oscilloscope simultaneously. Furthermore, it relies on using a power splitter/combiner, a Mini-Circuits resistive 50 Ω DC to 10000 MHz ZX10-14-S+, in order to divide the discharge signal from the CDM test head into two equal waveforms. Identical 20 dB attenuators are used on all scope channels. Figure 1 shows two versions of the usual cable connection between the CDM tester and the oscilloscopes, each with two cables connected at a baffle. The Intel cabling system uses a Mini-Circuits cable connected to a Sucoflex_126_e cable in contrast to the standard Thermo Fisher Scientific (Thermo) cables using two identical Mini-Circuits cables, with an SMA connector in both cases.

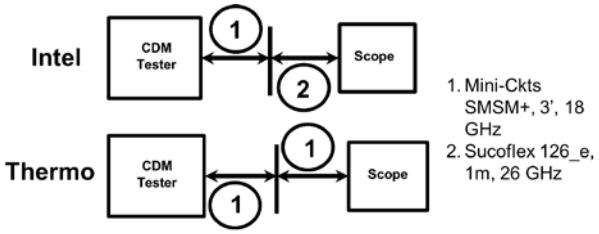

Figure 1: Sketches of configured CDM cable connectivity

Figure 2 depicts a setup in the lab for our promised studies of lossy cables. The cable from the CDM tester (Thermo Orion2) now ends at the power splitter, from which one output connects **directly** into scope Ch. 2, while the other output passes through another coaxial cable into Ch. 1.

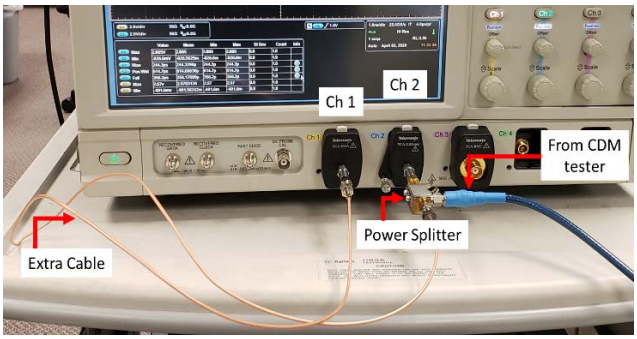

Figure 2: Experimental setup with configured cable connectivity

The two equal waveforms will thus experience no attenuation (Ch. 2) or attenuation due entirely to the extra cable of known fixed length (Ch. 1). The goal is to compare the waveform from a "*zero length*" un-attenuated connection (Ch. 2) to an attenuated waveform having passed through the coaxial cable of

fixed length, with attenuation due to known skin and dielectric losses. We carefully selected a coaxial cable and length so that losses would allow us to compare theory and experiment easily with pulse measurements. Considering repeatability and noise in the measurements, top of the line cables such as Sucoflex_126_e, while used in CDM testers, would not be a good choice for these studies. We therefore chose Pasternack RG316 and RG178 cables as our "lossy" cables.

III. Deducing Impulse Responses

Data sheets for many cables often have a very limited number of data points representing the attenuation vs. frequency. Curve fitting improves with more data, so having access to a vector network analyzer or equivalent, to measure the cable attenuation across frequency, will provide larger data sets for a much-improved curve fit. Figures 3 and 4 below show 2nd order polynomial fit to the square root of frequency for RG316 and RG178, respectively.

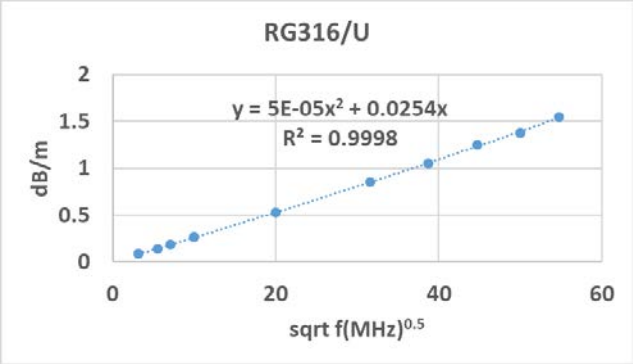

Figure 3: Attenuation vs. square root of frequency RG316

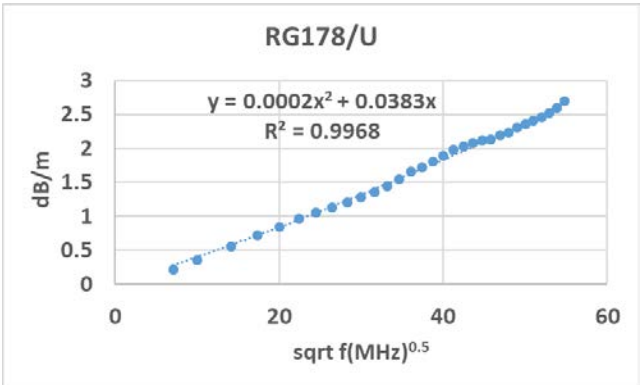

Figure 4: Attenuation vs. square root of frequency RG178

These losses, and others shown later, are taken from S21 data. The curves are not influenced by S11 reflections, as S11 was always below -20 dB. The constant parameters a and b in Equations 3 and 4 are extracted from the curve fitted equation shown in the figures, where a goes with the x term and b goes with the squared term. In both figures the goodness of fit (R^2) for the data is better than 99%. The a and b quantities also agree well with datasheet values, as expected. But for our 4-meter length of RG316/U cable, a and b from dB/m (Figure 3) must each be multiplied by 4 to give τ_1 and τ_2 in Equations 3 and 4, suitable for use as impulse responses in Equations 1 and 2. Using values from Figure 3 and scaling, we get τ_1=43.6 ps and τ_2=7.33 ps for the 4-meter length of RG316. This is quite enough to influence the measured waveform noticeably. Figure 5 shows the impulse responses of $h_1(t)$, $h_2(t)$ and $h_3(t) = h_1(t) \otimes h_2(t)$ for a 4-meter long RG316 coaxial cable.

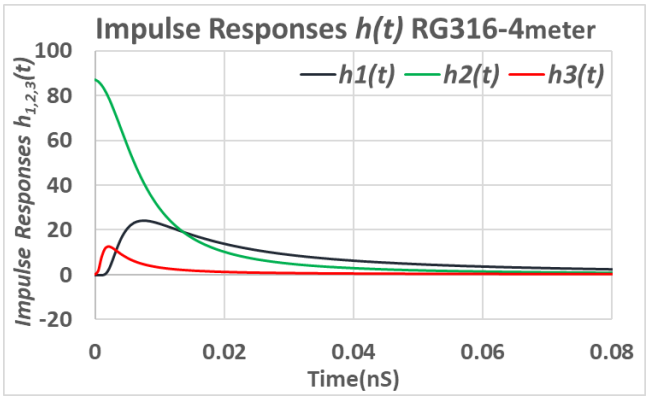

Figure 5: $h_1(t)$, $h_2(t)$, $h_3(t)$ impulse responses vs. time(nS)

IV. (De)Convolution process

$h_3(t)$ shown in Figure 5 is the result of numerical convolution performed using installed macros in Excel [7]. Using the macro "Convolve", $h_3(t)$ is found from numerical convolution of $h_1(t)$ and $h_2(t)$. At this point the impulse response $h_3(t)$ contains contributions from both $h_1(t)$ and $h_2(t)$. Convolving $h_3(t)$ with the CDM waveform directly connected to the scope (zero-length, as described above) results in a waveform that will be compared to that coming out of the fixed length coaxial cable, 4-meters long in this case. Given that CDM discharges are not totally repeatable and vary from one discharge to the next, each waveform to be compared with another comes from a single discharge and makes use of the splitter.

Figure 6, acquired using large verification module at 750V, compares the convolved (⊗) waveform as described above to that measured using a 4-meter long RG316 cable as well as a zero-length CDM reference measurement. Figure 6 is aligned to show only the relevant segments of the waveforms.

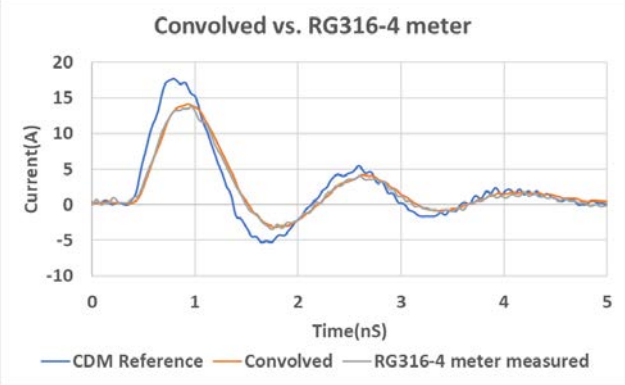

Figure 6: Convolved vs. 4-meter length and reference

What is shown in Figure 6, and significant, is that the convolved and 4-meter RG316 coincide in both amplitude and width. The peaks of the two waveforms and FWHM (full width at half maximum) align. For a large CDM verification module (CDM Tester Verification Module) [1] and 4-meter long RG316 cable, Figure 6 shows ΔIpeak/Ipeak~0.226. The convolution process is subsequently verified by performing a Deconvolution process using the macro "DeconvolveFT" from the installed macro bundle [7]. Figure 7 shows the result of deconvolving the measured waveform using $h_3(t)$, then comparing with the actual CDM reference waveform.

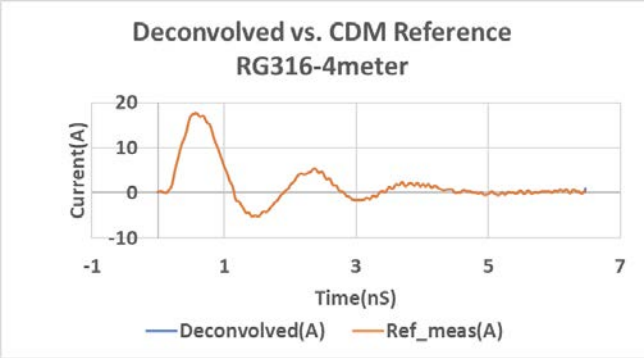

Figure 7: Deconvolved and CDM reference waveform; found to be coincident.

Figure 7 shows that the deconvolved and the CDM measured waveform (from a Mini-Circuits 50 Ω DC t-10000 MHz ZX10-14-S+ power splitter with two outputs (6dB)), also acquired using large verification module at 750V, exactly align. This result confirms the accuracy of the convolution process. Of course, the objective of this work for CDM testing is, ultimately, not to compute the effect of lossy cables, but to know the effect of cables that we use, as in [4]. The work in [4] started with analytically "reasonable" waveforms for the large CDM verification module and calculated the effect of two different cable sets, arriving at an anticipated measured waveform. The Intel cable set used in [4] (about one meter each of Mini-Circuits SMA and Sucoflex 104 cables) showed a 4.7% drop in peak current from tester to scope, and the Thermo cable set (two one-meter segments of Mini-Circuits SMA) a 6.4% drop. The waveform in [4] was a bit narrower than our present reference waveform in Figures 6 and 7.

When this reference waveform is deconvolved with present methods for the Intel cable set (the actual cables used to take the signal from the tester to the scope), the resulting waveform has an Ipeak 4.05% higher. The peak current correction for a Thermo cable set is 5.3%. This all makes sense given the higher tau (τ) values for the more flexible Mini-Circuits cable, and the slightly wider CDM reference waveform used in this work. Details are presented here, including a study relating peak current correction to CDM waveform width. This allows users to estimate the cable correction for a cable set without having to perform deconvolution each time.

V. Experiment & Results

Determining the actual discharge level at the CDM test head requires only the process of Deconvolution as described above. The process is to capture what is shown on the oscilloscope and deconvolve the two impulse responses of skin and dielectric losses, i.e. $h_3(t)=h_1(t) \otimes h_2(t)$ and the result is the identical waveform as shown on the scope with a larger magnitude essentially retrieving back what has been lost through the coaxial cable connection from the test head to the oscilloscope. Capturing the waveform from the oscilloscope is a trivial process while care must be given in determining an accurate $h_3(t)$. For the purposes of illustrating this process of deconvolution, only the Intel cabling system is shown, which is a Sucoflex_126_e, via an SMA connector, connected to a Mini-Circuits SMA-male/SMA-male CBL-3FT-SMSM+. Although the same process is equally applicable to any kind of a cabling system that may be used. Studies shown in this paper start out by capturing the attenuation vs. sqrt of frequency as was described in Figures 3 & 4 where now a VNA (Vector Network Analyzer) is used to capture the attenuation over a large frequency range and shown in Figures 8 and 9 for the Intel as well as Thermo cabling system, respectively.

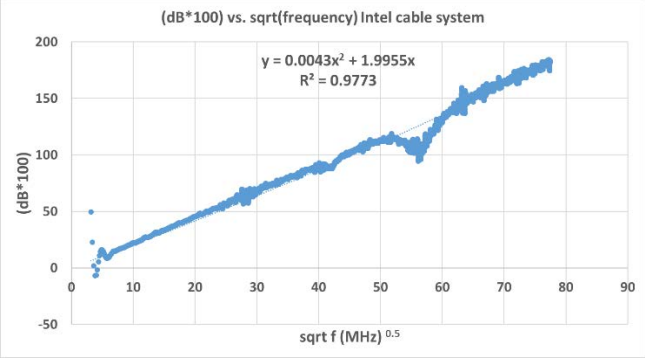

Figure 8: Attenuation vs. square root of frequency for Intel cable system

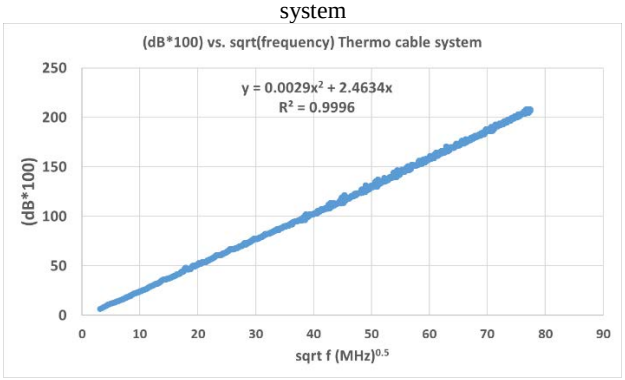

Figure 9: Attenuation vs. square root of frequency for Thermo cable system

The polynomial fit (using Excel) as described above produces the a & b coefficients. For these studies some of the behaviors observed are overlooked such as an apparent resonance (dip in the curve) at around 3 GHz which appears (from S11) to be due to slight reflections in the cables or connector. It should be noted that in order to get better numerical resolution in Excel during curve fitting, the attenuation data was multiplied by 100 and subsequently divided out for continued analysis. Using these coefficients, the tau (τ) values described in Equations 3 and 4 were determined to be τ_1=1.680 ps and τ_2=1.576 ps for the Intel cables while for the Thermo cables, τ_1=2.560 ps and τ_2=1.063 ps. It should be noted that the τ values are now based on the entire cable assembly including the SMA connector, in both cabling systems.

The overall length of the two cables together is approximately 2 meters. With the τ values calculated, the impulse responses $h_1(t)$ and $h_2(t)$ are determined. These two are convolved to give the 3rd impulse response $h_3(t)=h_1(t) \otimes h_2(t)$, a single function that captures both skin and dielectric losses in the cables, as discussed earlier, plus the in-between SMA connector.

$h_3(t)$ is now deconvolved from the actual measured data as captured by the oscilloscope using the Intel cabling system. As discussed above, this will be a waveform quite like what is shown on the oscilloscope, however exhibiting a larger magnitude. Figure 10 shows this comparison.

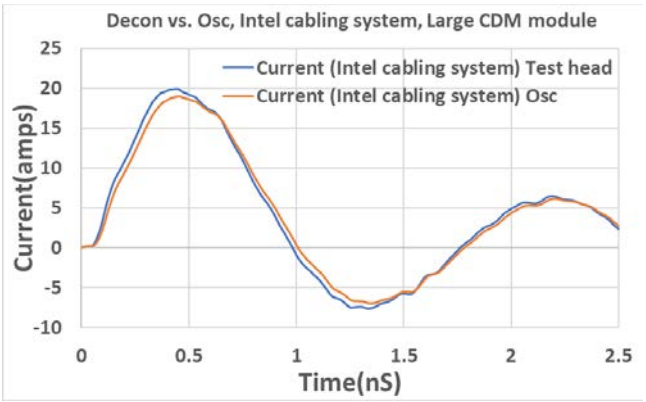

Figure 10: Intel cable set with oscilloscope vs. deconvolved waveforms, ***Large*** CDM verification module, JS-002

Figure 10 shows the waveform as captured by the oscilloscope vs. the same waveform after the process of Deconvolution, using a ***large*** CDM verification module as specified by JS-002. As is shown in Figure 10, the deconvolved waveform is larger as anticipated. For this example (+750V), the peak current as shown by the oscilloscope is about 19.015 amps while the deconvolved waveform is about 19.94 amps which is about a 4.8% change in peak current.

This describes that what the user was observing on the oscilloscope is 4.8% less than the actual waveform as discharged at the CDM test head. Figure 10 shows that in this case, the main effect of the Intel cabling system is amplitude loss, not width increase. Although both happen in a convolution operation, amplitude loss is most prominent for this impulse function and waveform.

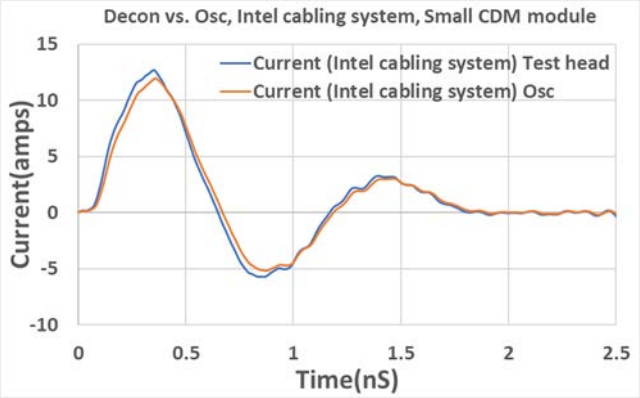

Figure 11: Intel cable set with oscilloscope vs. deconvolved waveforms, ***Small*** CDM verification module, JS-002

Figure 11 repeats the process as described above in Figure 10, however this time a small verification module [1] is used instead.

As is shown in Figure 11, the deconvolved waveform is larger, as anticipated. For this example (+750V), the peak current as shown by the oscilloscope is about 11.93 amps while the deconvolved waveform is about 12.67 amps which is about a 6.2% change in peak current. This describes that what the user was observing on the oscilloscope is 6.2% less than the actual waveform as discharged at the CDM test head. Figure 11, as in Figure 10, shows that in this case, the main effect (most prominent) of the Intel cabling system is amplitude loss, not width increase.

VI. Derived Correction Factors

The remainder of these studies focuses on creating a look-up graph for two main cabling configurations, the Intel cable system, composed of a Mini-Circuits SMA-male/SMA-male CBL-3FT-SMSM+ that is connected to a Sucoflex_126_e cable via an SMA connector, and the Thermo cabling system composed of two Mini-Circuits SMA-male/SMA-male CBL-3FT-SMSM+ connected together also via an SMA connector.

The goal is to provide users with a look-up graph determining the approximate peak current at the CDM test head, without having to perform the deconvolution process each time. Then by (a) using a look-up graph for approximating the actual test head currents, the user can (b) decide whether to use the methodology to find exact discharge currents at the test head, through the process of Convolution / Deconvolution. While the detailed methodology is more rigorous, the user would often like to assess an ROI (return on investment) for the effort, and the look-up graph can certainly help with that.

Look-up graphs as shown in Figures 12 and 13 are generated by using damped sinusoids [8] representing the CDM waveform with varying t_0, where t_0 represents the first half cycle or the time to the first zero crossing. The damped sinusoid closely represents CDM waveforms. Before and after convolution, we expect the peak current times t_0 to be very close to a constant, due to charge conservation and negligible loss at DC. Hence larger peaks (higher discharge currents) show a smaller t_0 and vice versa. Deconvolving $h_3(t)$, which in Figures 12 and 13 are for the actual Intel and Thermo cables using identical process described above, from a damped sinusoid (damping factor D=0.5, an arbitrary choice) produces another near-sinusoid that is larger in peak current as compared to the original waveform, also as described above.

The delta in peak current between the deconvolved and the damped sinusoid shows a loss in current across the cabling system; thus, a specified Imax multiplier can approximately correct the loss in current. Once completed across a range of frequency ($1/t_0$) the look-up graphs with multiplication (Imax-mult) factors suitable for CDM test head discharges result, as shown in Figures 12 and 13.

Users can collect a CDM waveform via an oscilloscope, measure the time to first zero crossing, compare to Figure 12 and read off the multiplication factor from the vertical axis.

Figure 12 shows three curves, representing a baseline that was generated using data sheet values as well as two other curves that represent the Intel and Thermo cabling system. The baseline curve (for the Intel cable system datasheet values) shows less loss than the measured data for cables plus connector, as expected. The plot also shows that the Intel cabling system has less loss than Thermo, as one would have anticipated using a higher performing cable such as Sucoflex_126_e.

Figure 13 shows how to transform Thermo data into Intel data. Figure 13 was generated with the ratio of curve fitted equations shown in Figure 12, showing a peak conversion factor of 1.016x. Thus, the two cable systems, no more than 1.6% apart, are reasonably aligned. The message of Figure 12 is that for sharp waveforms, Ipeak could be read out 12-14% low.

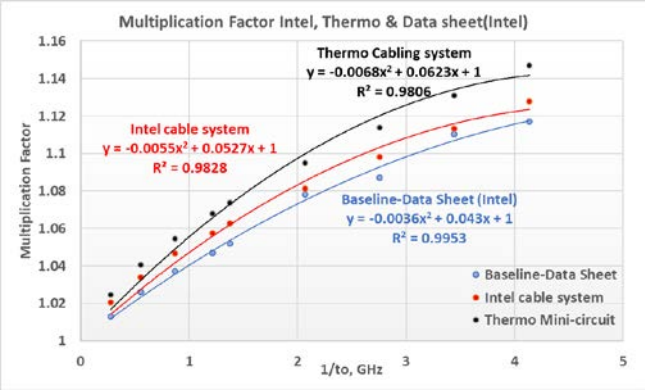

Figure 12: Imax multiplication factor vs. pseudo-frequency (γ_0), shown as $1/t_0$

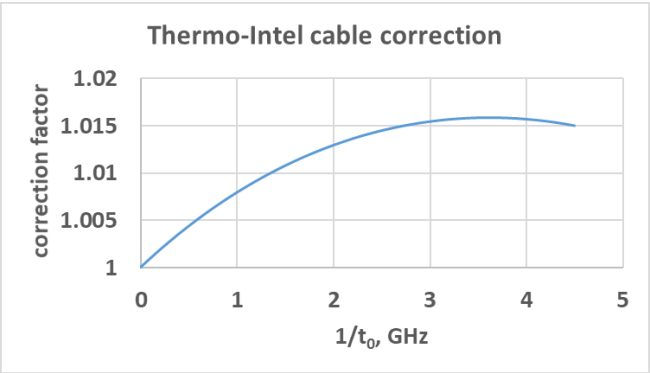

Figure 13: Imax multiplication factor transitioning between Thermo and Intel cable systems vs. frequency, where t_0 is the first zero crossing

Table 1 shows the Imax (Ipeak current resulting from the two verification modules) values using multipliers from Figure 12, comparing to those obtained using the (de)convolution methodology.

CDM Verification Module_JS-002	t_0 (nS) 1st zero crossing	γ_0 (GHz) Fig. 12	Multiplier	Imax Oscilloscope (A)	Imax_mult Fig.12 (A)	Deconvolved (A)
small	0.67	1.49	1.07	12.12	12.97	12.68
large	1.01	0.99	1.05	19.32	20.23	19.94

Table 1: comparing Imax using multiplier to (de)convolution methodology (using Intel cable system)

Table 1 compares small and large verification modules using the two methodologies. Using the time to 1st zero crossing, we can determine the pseudo-frequency γ_0 as shown in Figure 12 as $1/t_0$ on the horizontal axis. The parameter γ_0 results into the multiplier as shown on the vertical axis of Figure 12 multiplied by the measured Imax from the oscilloscope as shown under Imax_mult in Table 1. The deconvolved column in Table 1 reflects the same data but using the (de)convolution methodology. Some amount of discrepancy between Imax_mult and deconvolved columns are evident. These discrepancies can be dedicated to using the curve fitted equations of Figure 12 vs. the (de)convolution methodology. The difference between Imax_mult and (de)convolved for the small verification module is ~1.9% and for the large verification module is ~1.4%, where the Imax_mult is intended to represent an upper bound.

VII. Discussion and Conclusion

This work has shown how to anticipate, measure, and correct for the skin and dielectric loss effects in coaxial cables that carry the CDM test head signal to the oscilloscope. Starting with frequency domain loss data, the main loss effects can be sorted out and combined into a time domain impulse function for each cable set, a function that is convolved with (or deconvolved from) a measured waveform to include (or correct for) the losses in the cables. The analytic methods were cross-checked with experiments on long lengths of cable, showing extremely good agreement with theory. Fortunately, the datasheet loss values for off-the-shelf cables are usually good estimates of measured values and are sufficient to drive a cable choice for meeting the requirements of JS-002 [1], although a VNA measurement of the final cable assembly is always preferred. Our work concludes with application of the methods to cable assemblies used for CDM testing (Intel and Thermo), plus a summary lookup chart, suitable for everyday use with those cable sets. Losses for the CDM verification targets of JS-002 [1] are mild,

but corrections for very small devices or small experimental metal targets could be 12-14%. In conclusion, the methodology of applying two-parameter (de)convolution to determine the performance of coaxial cables used in CDM discharges is viable. Application of these corrections should be made under the guidance of JS-002 committee (ESDA /JEDEC JWG on CDM) which incorporates cable losses in existing specifications. The most useful application of these corrections is for determining the actual Ipeak that a product experiences under CDM discharges for better alignment with simulations, design planning, as well as fault analysis and isolation.

As discussed in the Introduction, the cable losses of this work are the second of three major elements of the CDM measurement channel that take the device current information from device to oscilloscope. Oscilloscopes were considered some time ago [2]; with a fast-modern scope the waveform corrections can now be minimal to negligible. On the other side of the cables is the CDM test head, essentially a ~1 ohm current-sensing resistor, but the assembly has some kind of bandwidth (due to capacitance from probe to upper ground plate, for example) and transfer function that would extract on-chip device current Id(t) from output voltage Vout(t), i.e., a trans-admittance function. This is yet another filter and something to be deconvolved from the measured waveform, once it is corrected for scope and cable loss. Despite detailed studies of the CDM hardware [9,10], nobody has yet proposed such a trans-admittance impulse function for the test head. When that happens, we would be prepared to combine it with the other two elements and assess the full impact of the CDM measurement channel on our understanding of the CDM device current.

Acknowledgements

The authors would like to thank Josh P. Morris, Sean Lynch, Greg Larson and Brett Carn for their help on CDM and cable loss measurements.

References

[1] ANSI/ESDA/JEDEC JS-002-2018, Charged Device Model (CDM)-Device Level test standard, Dec. 2018. See www.esda.org.

[2] T.J. Maloney and A. Daniel, "Filter Models of CDM Measurement Channels and TLP Device Transients", 2011 EOS/ESD Symposium Proceedings, pp. 386-394. See https://sites.google.com/site/esdpubs/documents/esd11.pdf.

[3] T. Maloney, "Skin-depth Losses in Measurement Cables and Their Effect on CDM Waveforms", IEW2017. See https://sites.google.com/site/esdpubs/documents/IEW17-tjm-complete.pdf.

[4] T. Maloney, "A Turnkey Method for Calculating Coaxial Cable Loss Effects on CDM Waveforms", EOS/ESD Symposium 2018. See https://sites.google.com/site/esdpubs/documents/esd18.pdf.

[5] R.B. Wu, Fast Eye-Diagram Analysis, Jan. 2017. See http://cc.ee.ntu.edu.tw/~rbwu/rapid_content/course/highspeed/SI11_Fast_Eye.pdf. Simple causal form for dielectric loss impulse function, Jan. 2017.

[6] R.L. Wigington and N.S. Nahman, "Transient Analysis of Coaxial Cables Considering Skin Effect", Proc. IRE, vol. 45, pp. 166-174, Feb. 1957.

[7] Web resource, "Excellaneous" VB macros; see MacroBundle12 a. http://www.bowdoin.edu/~rdelevie/excellaneous/#downloads

[8] T. Maloney and Nathan Jack, "CDM Tester Properties as Deduced from Waveforms" 2013 EOS/ESD Symposium, paper 9A.1, pp. 374-382 See https://sites.google.com/site/esdpubs/documents/esd13.pdf.

[9] J. Barth, L.G. Henry, and J. Richner, "Improving CDM Measurements With Frequency Domain Specifications", 2016 EOS/ESD Symposium Proceedings, paper 4A.1.

[10] F. zur Nieden, K. Esmark, S. Seidl, and R. Gärtner, "Predict the Product Specific CDM Stress Using Measurement-based Models of CDM Discharge Heads", 2016 EOS/ESD Symposium Proceedings, paper 4A.3.